ELSEVIER

Simulation of gas injection into liquid melts

M. P. Schwarz

CSIRO Division of Minerals, Clayton, Victoria, Australia

Gas injection is used in several metal smelting and refining operations to increase mixing in the melt and as a carrier for particle addition. Some of the fluid dynamical phenomena that occur in liquid baths when injected with gas are discussed. Mathematical models for simulating three of these phenomena are described: a two-fluid model for simulating bath circulation is compared with data obtained in air–water experiments; a technique that allows the swelling of the bath surface to be simulated is illustrated; and a mathematical model for the prediction of wave motion in gas-agitated baths is summarized.

Keywords: gas injection, two-phase, bubble plume, wave motion, numerical simulation

1. Introduction

Gas injection is used in many metallurgical smelting and refining operations to increase mixing in the melt and as a way of adding particles. For example, bottom blowing of oxygen is an important part of the present day steel converter operation; ladle treatment of hot metal and steel such as dephosphorization, desulphurization, and alloying utilize gas stirring to improve mixing, and many nonferrous processes such as the Noranda process, Peirce-Smith converters, and Sirosmelt incorporate submerged injection of gas.

The present trend in metallurgical processing is toward higher rates of gas injection, because this allows higher process intensity to be achieved, i.e., higher productivity per unit volume of vessel.[1] Examples of very high intensity processes being presently developed are the new bath-based processes for ironmaking,[2] e.g., The HIsmelt Process,[3] and the DIOS process.

Computational fluid dynamics can assist in the development of these new metallurgical processes,[4] but it is necessary to have a reasonably fundamental understanding of the flow phenomena of importance to the process. Mathematical modelling provides both a framework for developing this understanding, and a tool for applying the understanding to assist process development.

In this paper, mathematical models for simulating three of these phenomena are described: a two-fluid model for simulating bath circulation is compared with data obtained in air–water experiments; a technique that allows the swelling of the bath surface to be simulated is illustrated; and a mathematical model for the prediction of wave motion in gas-agitated baths is summarized.

Simulation of turbulent gas–liquid two-phase flows is an area at the forefront of current fundamental research. This is mainly because of inadequacies in the current state of turbulence models for such flows and because of the complex interactions that can occur between gas bubbles and the bulk liquid. Simulation techniques must therefore be checked by comparing predictions with data from well-controlled experiments. Some of the validation tests undertaken using data from air–water systems will be described. The issues involved in mathematical modelling gas injection will be addressed in a generic way; models for particular processes will not be dealt with.

2. Dynamics of liquid baths with gas injection

Figure 1 illustrates the main elements of gas injection as used in metallurgical processes. We will use this simplified case of bottom injection of gas into a cylindrical vessel as a basis for our discussion, though in real processes the bath geometry may be different, gas injection may be through multiple nozzles and may be from the side or top as well as from the bottom. Although these complexities may add to the difficulty of modelling the process, the basic phenomena and the simulation of them can be discussed with reference to the generic set-up shown in *Figure 1*.

The dynamics of a bath into which gas is injected is complex and no mathematical model is capable of simulating all the phenomena in detail. First, a large range of length scales is involved: on the bubble length scale there are processes such as bubble coalescence and breakup, whereas from the point of view of the bath length-scale, the details of flows around and within individual bubbles may not be important.

Address reprint requests to Dr. M. P. Schwarz at the Division of Minerals, CSIRO, RMDC Box 312, Clayton, Victoria 3169, Australia.

Received 29 November 1993; revised 14 December 1994; accepted 16 January 1995

655 Avenue of the Americas, New York, NY 10010

0307-904X/96/$15.00
SSDI 0307-904X(95)00109-W

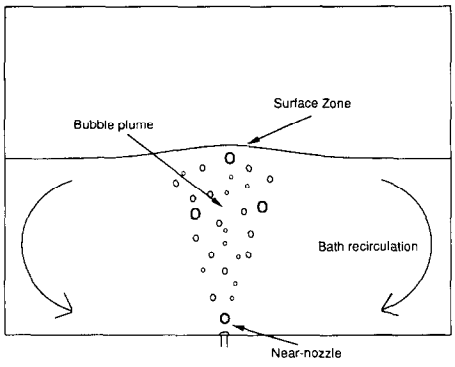

Figure 1. Simplified cylindrical geometry used for discussion of gas injection.

Second, the phenomena occurring in the bath change depending on the flow rate of gas injection, the mode of gas injection, the bath depth, etc. For very low gas flow rates, the bubble plume consists of well defined individual bubbles which do not interact greatly with each other. This can be referred to as the bubble regime. As the rate increases, the bubbles interact more and more and the plume becomes more turbulent. Both of these trends lead to continuous break-up and coalescence of bubbles as they ascend in the bath. This regime is usually referred to as the churn-turbulent regime.[5]

As the gas rate is increased further, the flow changes yet again. Intermittent channelling of gas through the bath can occur if the bath depth is shallow enough.[6,7] Blow-through or jet penetration has been used as a term to describe this extreme condition. In very shallow baths a similar situation is described as a spray regime.[8]

It is important to recognize that the mechanisms governing the gas–liquid interactions are different in these three regimes. In building a simulation model which is predictive, one aims to represent these mechanisms in a way that is as fundamental as possible. Nonetheless, given the complexity of the interactions, they will need to be described at some level by empirical relationships. One must be careful not to apply mechanistic descriptions or empirical relationships that have been obtained for one regime to a different regime where the relationships may not apply.

3. Phenomena in gas-agitated baths

Because it is impossible at present to build a simulation model that accurately describes all phenomena occurring in a gas-agitated bath (i.e., at all length scales, in all possible flow regimes, etc.), it is useful to identify the phenomena that are important for the industrial process being studied before embarking on a model-building exercise. Phenomena that occur in a gas-agitated bath can be conveniently classified according to general location: near-nozzle, gas–liquid plume, surface, and whole bath. Of course there is inevitably interaction between phenomena occurring in different parts of the bath, but the division is useful in understanding which are important for the industrial process being studied. It is also necessary to isolate individual phenomena using well-defined experiments in order to obtain a fundamental understanding of the phenomena and to develop empirical relationships necessary to describe the phenomena within the simulation model.

3.1 Near-nozzle

At low gas rates individual bubbles form at the nozzle and periodically detach, whereas at high flow rates the gas exiting the nozzle forms a jet that penetrates a certain distance into the liquid before breaking up into bubbles. Much work has been done on both regimes and on identifying a criterion for the transition from one to the other, the so-called bubbling-jetting transition.[9] The near-nozzle phenomena are also influenced by cross-flow, the direction of injection (up, down, or side), and mode of injection (e.g., through a nozzle or a porous plug).

3.2 Gas–liquid plume

Mention has already been made above of three regimes of injection, which were primarily distinguished by the topology of the interfacial surface within the gas–liquid plume (e.g., noninteracting bubbles, voids, etc.). The structure of the voidage and interfaces in the churn-turbulent and blow-through regimes has received little study. There is a strong interaction between this structure and turbulent eddies, and the chaotic nature makes this a complex problem to treat in detail. Most mathematical modelling seeks a time and space averaged solution using empirical constitutive relationships to take account of the small-scale phenomena.

3.3 Surface

The flow dynamics at the surface may be important for several reasons. Sometimes a jet of reactive gas is blown onto the surface as in combined blowing steel making, and then mass transfer across the surface is affected by the flow of gas across the surface. A lighter liquid (e.g., a slag) will float as a layer on the surface and may affect the bath dynamics. Perhaps the most important phenomenon at high gas flow rates is the formation of splash in the region where gas leaves the bath. Another surface-related phenomenon is large-scale wave motion. This slopping motion is treated in more detail in a separate section below.

3.4 Whole-bath phenomena

The most important of these is the large-scale recirculation set up by the upward motion in the plume (*Figure 1*). The importance of this recirculation in industrial processes is that it controls mixing through the bath. Gas injection is often used to promote mixing, for example when powders are added to melts as in ferrous ladle metallurgy. The bulk flow velocities are also important if there are two liquid phases (e.g., slag and metal) and the rate of mass transfer between the two is influenced by the velocity near the interface. Many studies have been reported in which mix-

ing times have been measured for such situations.[10] Modelling of the recirculation will be discussed in more detail later.

The remainder of this paper will be devoted to discussing the simulation of three aspects of bath dynamics in greater detail: bath circulation, surface swelling, and wave motion.

4. Bath recirculation

The bulk recirculation in a bath with gas injection can be solved with a two-fluid (or two-field)[11] technique or by using Lagrangian particle tracking for the dispersed gas phase.[12] The two-fluid method has a decided advantage over the particle tracking technique if the volume fraction of the dispersed phase is significant, because all published particle tracking methods assume negligible dispersed (bubble) phase volume fraction in the Eulerian liquid phase part of the calculation. Other simpler techniques have been used,[13,14] but they generally do not solve for the spatial gas distribution. In the two-fluid method, both gas and liquid phases are treated mathematically as continua, and the governing equations are derived by averaging over the small-scale structure (i.e., bubbles). The equations solved are:

$$\nabla\cdot(R_l\mathbf{v}_l) = \nabla\cdot(D_t\nabla R_l) \tag{1}$$

$$\nabla\cdot(R_g\mathbf{v}_g) = \nabla\cdot(D_t\nabla R_g) \tag{2}$$

$$\nabla\cdot(R_l\rho_l\mathbf{v}_l\mathbf{v}_l) = \nabla\cdot(\mu_{eff}R_l\nabla\mathbf{v}_l) - R_l\nabla p + \mathbf{F}_f + \mathbf{F}_l \tag{3}$$

$$\nabla\cdot(R_g\rho_g\mathbf{v}_g\mathbf{v}_g) = \nabla\cdot(\rho_g\nu_{eff}R_g\nabla\mathbf{v}_g) - R_g\nabla p - \mathbf{F}_f - \mathbf{F}_l - R_g(\rho_l-\rho_g)\mathbf{g} \tag{4}$$

with

$$\mu_{eff} = \mu_l + \mu_t \tag{5}$$

and

$$R_l + R_g = 1 \tag{6}$$

The pressure is considered to be common to the two phases, and both gas and liquid are assumed to be incompressible. The gas phase effective (kinematic) eddy viscosity, ν_{eff}, is taken to be equal to the liquid phase value, μ_{eff}/ρ_l, though in most cases the results are insensitive to its value because of the relatively strong coupling of the gas and liquid phase velocities through interphase friction. A review of the equations of two-phase flow has been given by Stewart and Wendroff.[15]

The interphase interaction effects are complex, depending as they do on small scale structure not resolved in the computation. The small scale structure includes phase structure (i.e., bubbles and their break-up and coalescence) and velocity structure (i.e., turbulence, bubble wakes, etc.) and the two interact (e.g., bubbles affect the liquid phase turbulence structure). Although the interaction terms can be derived in principle by averaging over exact equations, in practice empirical input is required. The usual practice is to capture all the complex physics of the small-scale phenomena within a small number of terms that specify overall interphase interaction effects. These effects include turbulent interdiffusion of the phases, interphase friction, other forces such as the lift force on the bubble due to the velocity shear in the liquid, and liquid phase turbulence modulation by the bubbles.

Turbulent interdiffusion of phases is difficult in practice to separate from other sources of phase dispersion. For example, even a single bubble rising in a liquid with zero velocity shear can still move laterally: its motion is zig-zag or helical and is related to the wake shed by the bubble.[16] In a bubble swarm, and in the presence of turbulence, this motion would be randomized and would result in additional interdiffusion of the phases.

Two approaches to phase interdiffusion have been used by this author with very similar results. It can be modelled by turbulent diffusion with diffusivity, $D_t = \mu_t/\rho_l$ plus a transverse "lift" force on bubbles. The lift coefficient, C_l, in the expression for the transverse lift force,[17] of which the dominant radial component is modelled (following Davidson[18]) as

$$F_{l_r} = C_l\rho_l R_l R_g(W_g - W_l)\frac{\partial W_l}{\partial r} \tag{7}$$

can then be fitted to give the measured plume spreading. Alternatively, an additional empirically determined component, D_a, can be added to the turbulent diffusivity: $D_t = \mu_t/\mu_l + D_a$. C_l is found to be between 1 and 1.5 and D_a about 0.01 m^2/s. Note that the diffusion terms in the continuity equations (1) and (2) that model interphase diffusion of bubbles through the liquid may alternatively be represented by force terms in the momentum equations[18].

The interphase friction term is calculated in the present work as

$$\mathbf{F}_f = C_f R_l R_g(\mathbf{v}_g - \mathbf{v}_l) \tag{8}$$

where $C_f = 4\times10^4$ $kg/m^3/s^1$. This value corresponds to a slip velocity between gas and liquid phases of 0.25 m/s. This is a good approximation to the experimentally determined terminal velocity in water of single air bubbles of diameter between 1 and 10 mm.[19] The slip velocity is almost constant over this range of diameters because of increasing nonsphericity as the diameter increases. For this reason equation (8) with constant C_f gives a much better representation of the friction over this diameter range than does the formula for drag on a sphere.

The effective eddy viscosity, μ_{eff}, is computed from the averaged velocity fields using the standard two-equation k-ϵ turbulence model[20]:

$$\mu_t = C_\mu\rho_l k^2/\epsilon \tag{9}$$

where the equation expressing conservation of either k or ϵ (ϕ say) is

$$\nabla\cdot(R_l\rho_l v_l\phi) = \nabla\cdot\left(\frac{\mu_{eff}}{\sigma_\phi}R_l\nabla\phi\right) + S_\phi \tag{10}$$

where

$$S_k = R_l(G_k - \rho_l \epsilon) + S_b \tag{11}$$

$$S_\epsilon = R_l \frac{\epsilon}{k}(C_1 G_k - C_2 \rho_l \epsilon) \tag{12}$$

and

$$G_k = \mu_t \left\{ 2\left[\left(\frac{\partial W_l}{\partial z}\right)^2 + \left(\frac{\partial V_l}{\partial r}\right)^2 + \left(\frac{V_l}{r}\right)^2 \right] + \left(\frac{\partial W_l}{\partial r} + \frac{\partial V_l}{\partial z}\right)^2 \right\} \tag{13}$$

The standard values,[20] $C_1 = 1.44$, $C_2 = 1.92$, $C_\mu = 0.09$, $\sigma_k = 1.0$, $\sigma_\epsilon = 1.3$, are used for the empirical constants.

The term for the source of bubble-induced turbulence, which we model with a generalized form of the expression used by Johansen and Boysen [12],

$$S_b = C_b \rho_l R_g (\mathbf{v}_g - \mathbf{v}_l)^2 \tag{14}$$

has little effect on the simulations presented in this paper but is important for higher gas flow rates and is needed to stabilize the computation when fine cells are used to resolve the region near the nozzle.

To solve these equations, we have employed the general purpose flow simulation package PHOENICS. The discretized forms of the equations (the finite domain equations) are obtained by expressing conservation of mass, momentum, and energy for each control cell or subdomain of a grid, and the formulation is fully implicit and conservative. The so-called IPSA algorithm is used to solve the discretized equations. Details of the solution procedure can be found elsewhere.[21]

Boundary conditions are applied by adding sources or sinks for the particular variable; however, they are described here in the conventional way. At $r = 0$ (the axis of symmetry), derivatives of all variables are set to zero. On the walls and the bottom of the vessel, standard wall functions are used to calculate the friction and the near-wall values of k and ϵ.[22]

For simplicity, we initially assume the top free surface of the bath to be flat and coincident with the upper boundary of the computational domain. We therefore allow no flow of liquid across the upper boundary, i.e., $W_l = 0$. Gas is allowed to leave through the surface at a rate given by the natural boundary condition,

$$\frac{\partial W_g}{\partial z} = 0 \tag{15}$$

In addition, the following conditions are applied at the surface:

$$\frac{\partial V_l}{\partial z} = 0 \qquad \frac{\partial k}{\partial z} = 0 \qquad \frac{\partial \epsilon}{\partial z} = 0 \tag{16}$$

4.1 Comparison with experimental recirculation

The technique has been tested against several sets of data obtained for air–water systems. We first discuss simulations of an experiment performed by Grevet et al.[13] in which velocities were measured in the bulk of the bath. This experiment has previously been simulated by a variety of methods.[13,23]

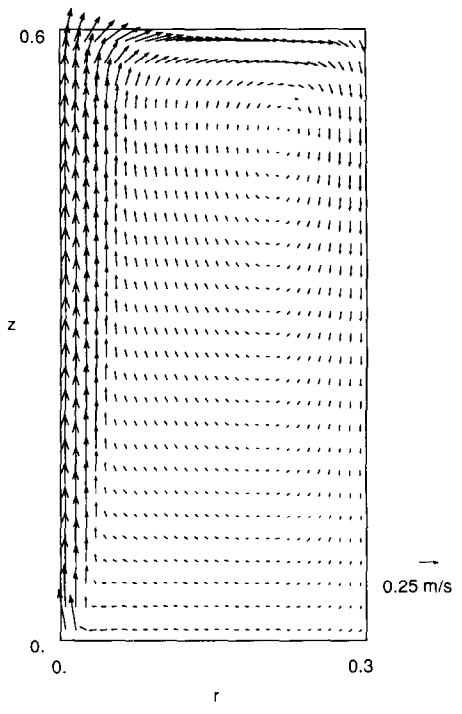

Figure 2. Computed flow-field for the experiment of Grevet et al.[13].

In the experiment, air was injected through a nozzle in the center of the bottom of a cylindrical tank, 0.6 m in diameter, filled with water to a depth of 0.6 m. The orifice diameter was 0.0127 m and the air velocity was 1.62 m/s and 3.2 m/s. Velocities and turbulence characteristics were measured with a laser Doppler anemometer.

Figure 2 shows the computed flow field for the 1.62 m/s case. Velocity vectors are shown on a vertical plane extending from the vessel axis ($r = 0$) to the outer wall ($r = 0.3$ m). The center of the vortex in *Figure 2* is in the same position as determined experimentally, and the high velocity stream that flows radially outward just below the bath surface and then down the top part of the outer wall is also seen in the data. The behavior of the plume impinging on the bath surface (from below) is somewhat analogous to a jet impinging on a wall: the stream attaches to the bath surface just as a jet attaches to a wall.

Detailed comparisons between the measured and computed velocities and turbulence energies for the 1.62 m/s case are given in *Figures 3a* and *3b* for profiles across the bath at the heights shown. The agreement in velocity is good although the turbulence level near the surface of the bath is overestimated typically by about 50% and by as much as a factor of three at one point. This same trend has been found in other simulations of gas-stirred baths.[24] The cause is possibly the strong curvature of the streamlines around the center of the vortex; the k-ϵ model is known to overpredict turbulence strength in strongly curved flows. In addition, small eddies will be damped by surface ten-

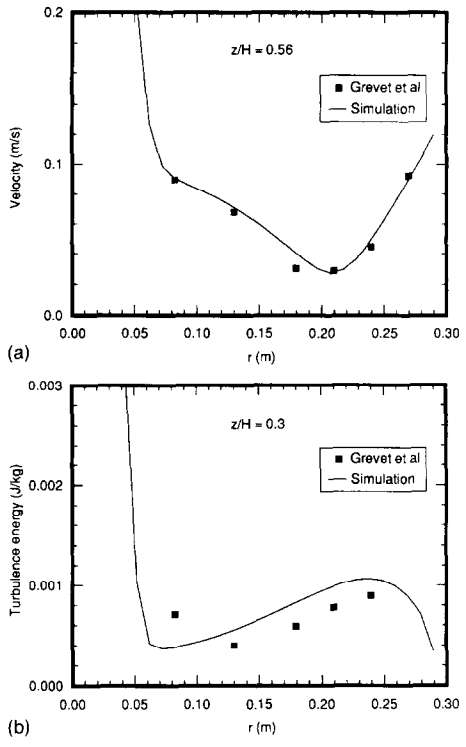

Figure 3. (a) Computed and measured liquid velocity magnitudes for the experiment of Grevet et al.[13] plotted against radial position in the bath. (b) Computed and measured turbulence energies for the experiment of Grevet et al.[13] plotted against radial position in the bath.

sion at the surface. The predicted velocity and turbulence level both increase sharply toward the center-line as shown in *Figures 3a* and *3b*, though data are not available at the plume axis to validate the predictions. Measurements are hard to make near the center-line because the high bubble concentration causes a low sample rate in laser-based techniques and may also result in severe biasing problems.[25] Measurements are further complicated by the plume rotation described below.

4.2 Comparison with void fraction measurements

To test whether the two-fluid model predicts the correct flow-field and structure in the two-phase region of the bath, we have used data collected by Castillejos and Brimacombe.[26] In their experiment, air was injected into a cylindrical vessel of diameter 500 mm filled with water. Six different sets of conditions were examined, but we concentrate on the case in which the bath depth was 400 mm, the nozzle diameter 6.35 mm, and the gas flow rate 876 N cm^3/s.

Castillejos and Brimacombe[26] used an electroresistivity probe to measure local void fraction within the gas–liquid plume. An annular baffle was placed just above the bath surface to damp out wave motion which would build up if the surface were free. This motion is a serious complicating factor for simulation because the gas–liquid plume precesses (or rotates) around the bath in synchronism with the wave. The effective time-averaged width of the plume would then be much greater than the instantaneous width, and the time-averaged velocity on the bath axis would be smaller than the velocity at the plume centreline.[25,27] Of course in real processes involving injection, the wave motion is not usually damped out, but it is still often important to know the plume centerline values of velocity and void fraction.

Figure 4 compares computed and measured void fraction profiles across the plume at three different heights, z, in the bath. The agreement is in general excellent, although the centerline void fraction is overestimated in the upper part of the bath. This is likely to be due to plume "wander," which cannot be taken into account in a realistic way by bubble diffusion or lift force (the only mechanisms in the model by which gas is spread out horizontally). Although the periodic rotating motion of the plume

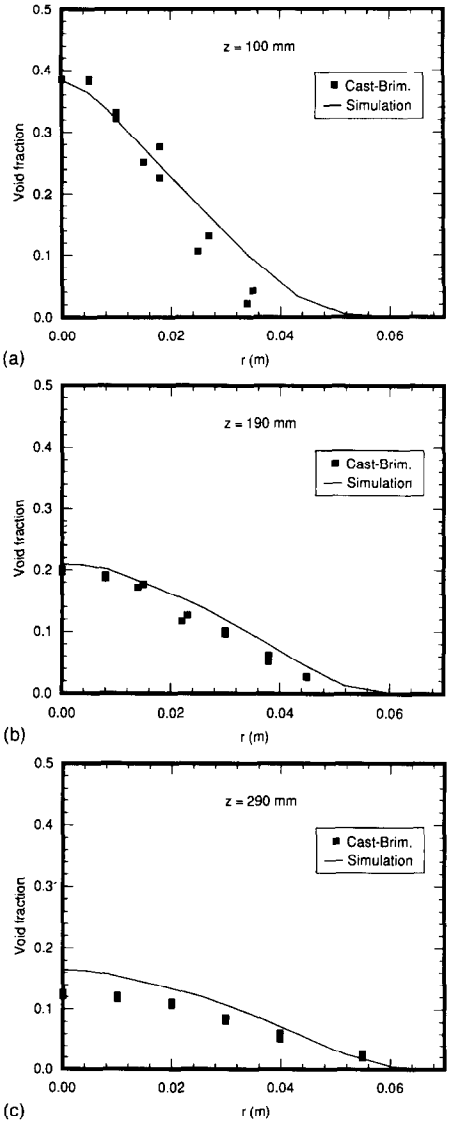

Figure 4. Computed and measured void fraction profiles across the plume at three different heights, z, for the experiment by Castillejos and Brimacombe[26].

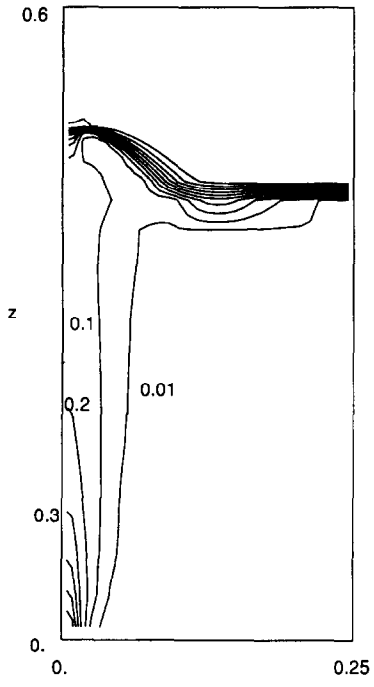

Figure 5. Computed void fraction distribution for the experiment by Castillejos and Brimacombe[29]. The computational domain includes both bath and gas space above it.

associated with sloshing was prevented by the presence of baffles, random plume wander still occurs.

5. Simulation of surface swelling

As indicated diagrammatically in *Figure 1*, the surface of the bath swells in the region where the plume reaches the surface. The swelling is one of the most obvious visual features of gas injection (particularly with a nontransparent liquid) and would be expected to have some influence on bath circulation.

One method for simulating the swelling that immediately suggests itself is to extend the two-fluid model introduced above so that the computational domain incorporates both the bath and the gas space above it. Such a simulation is illustrated in *Figure 5* where the Castillesjos and Brimacombe experiment[26] is once again simulated. Interphase diffusivity, D_t, is set to zero near the free surface to maintain as sharp an interface as possible. The height of the swelling is in accordance with measurements by Sahajwalla et al.[28]

When this technique is applied to a similar experiment by Anagbo and Brimacombe[30] in which bath circulation was measured, the predicted velocities near the tank wall are too low and the center of the recirculation cell is too far from the wall. Spurious vertical motion induced in the partially filled cells at the free surface affects the narrow horizontal stream that normally flows across the bath just under the surface (*Figure 2*). This spurious vertical motion can be easily understood by an analysis of the numerics pertaining to partially filled surface cells. The author believes that this effect is the reason for the unusual flow fields obtained by Turkoglu and Farouk[31] using a similar technique. Ironically, downward vertical velocities somewhat similar to the spurious ones do actually occur at higher gas flow rates as a result of droplets returning to the surface. The effect of these droplets is qualitatively similar[24] in that they reduce the recirculation velocity; however, one should be careful not to equate the two phenomena.

To circumvent this problem, the simulation was performed with a technique in which the computational domain contains only the bath but in which the top boundary of the domain is deformed to the shape of the swelling. The flow field shown in *Figure 6* is a more accurate representation of the recirculation based on the results of Anagbo and Brimacombe and other workers. In the case shown, the surface shape was taken from the previous "bath-plus-gas-space" model, but it can also be obtained by iterative adjustment of the shape until the pressure is constant over the surface.

Besides giving a less accurate representation of the bath circulation, another disadvantage of the bath-plus-gas-space technique is that it requires much more CPU time, since it must be run as a real transient with quite short time steps.

6. Wave motion modelling

Injection of gas into a bath of liquid can cause a wave or oscillation to be set up in the body of liquid, and this

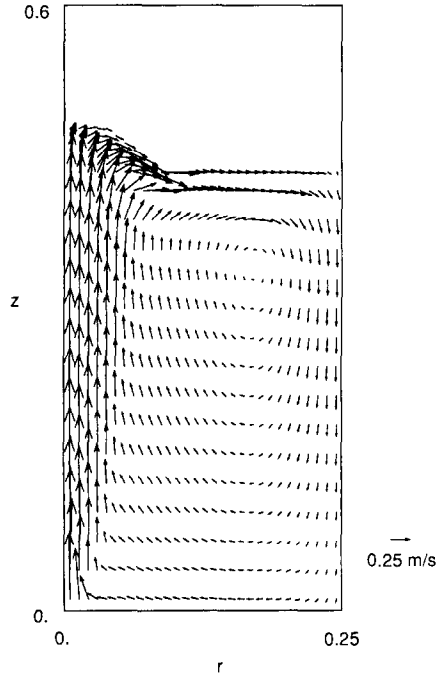

Figure 6. Computed flow field for the experiment by Castillejos and Brimacombe[29]. The free surface is treated with a deformed computational domain boundary.

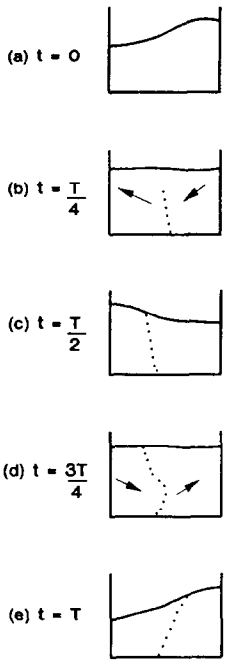

Figure 7. The evolution of an initial disturbance to the surface of a bath, and the effect of the resultant liquid velocity on the position of a bubble plume.

phenomenon is important in pyrometallurgical processes using gas injection. For example, in a bottom-blown steel converter, large amplitude slopping can result in melt loss and vessel vibration. The exact shape and amplitude of the wave motion depends on several factors: the gas flow rate, the tank geometry, the injection geometry, and the bath depth. For example, in an upright cylindrical tank (in some ways similar to the geometry used in OBM steelmaking converters) injection through a nozzle centrally placed in the bottom results in a rotating wave if the gas rate is sufficiently high.[32,33] In all cases, wave excitation only occurs for certain ranges of bath depth, so that the phenomenon appears to be some sort of resonance.

The author has proposed a mechanism[34,35] to explain the wave excitation according to which the buoyancy force on bubbles that are displaced from the center line as a result of the oscillation is sufficient to sustain the oscillation under certain conditions. Interaction between the plume motion and wave motion was analyzed theoretically to determine an equation for the evolution of any particular mode of oscillation and hence an expression for the amplitude of the wave excited.

The mechanism can be described without loss of generality with reference to a simple rectangular geometry. Consider a long rectangular tank with injection through a line of nozzles bisecting the tank: this reduces the problem to two dimensions. Above the nozzles, a plume containing a mixture of gas bubbles and liquid will rise to the surface. If the plume is displaced to one side of the centerline, the surface of the bath is raised on that side. There is then a restoring force (gravity) that moves liquid from the right-hand side of the bath to the left-hand side. In the absence of the plume, the bath, if initially disturbed to such a position, would oscillate back and forth, the amplitude decreasing with time because of damping. The presence of the plume leads to a selfsustaining oscillation.

Consider the disturbance shown in *Figure 7a* as an initial condition. The evolution of this disturbance is such that the liquid moves from the right-hand side to the left as shown in *Figure 7b* everywhere in the bath. This moves the plume to the left, and importantly, it moves any bubbles released at the nozzle to the left-hand side of the bath. All the bubbles released while the liquid is moving to the left end up in a plume on the left of center, and this displaced plume tends to reinforce the deformation (the rise in the surface level) on the left-hand side resulting from the free oscillation. The strength of the reinforcement depends on the number of bubbles released since the bath started moving to the left. The more bubbles, the greater the buoyancy force tending to raise the liquid on the left side of the tank.

There is a second important effect to be considered. This effect is related to the length of plume released during one half cycle. If the plume reaches all the way to the surface at the end of the first half cycle, all those bubbles will leave the bath during the next half cycle, and a new line of bubbles reaching to the surface will be created. At the end of the second half cycle, each of these new bubbles will have been moving to the right all their life. Therefore, the displacement of the plume to the right at the end of the second half cycle will be in some sense maximal.

On the other hand, if the line of bubbles created during the first half cycle only reaches half way to the surface, those bubbles are likely to remain in the bath during the next half cycle. Because they moved to the left during the first half cycle, their displacement to the right at the end of the second half cycle will not be maximal. In other words, the reinforcement of the wave by the buoyancy force will not be as great as it could be.

As a result, maximum reinforcement of the free oscillation is expected to occur when the transit time of bubbles through the bath is about one half of the free oscillation period; then a complete line of bubbles reaching all the way to the surface will be formed on the left side of the tank before the free oscillation moves the liquid back to the right-hand side.

7. Mathematical model of wave excitation

A brief summary of the mathematical model developed to describe the wave motion follows. The wave amplitude is described by a model involving a single degree of freedom:

$$\ddot{\phi} + \omega^2\phi = \mathscr{F} - \mathscr{D} \qquad (17)$$

where ϕ is the instantaneous amplitude of the mode of the surface deformation being considered. The amplitude, ϕ, will be measured as the displacement of the free surface from equilibrium at an antinode (i.e., at the vessel wall).

The two terms on the left-hand side of equation (17)

represent the free oscillation terms. For the fundamental, the period, T, is given by[36]

$$\omega^2 = \left(\frac{2\pi}{T}\right)^2 = \frac{\pi g}{l}\tanh\left(\frac{\pi H}{l}\right) \tag{18}$$

for a rectangular bath of length l and depth H.

The first term on the right-hand side of equation (17) represents the forcing due to the bubble displacement. The buoyancy force on bubbles displaced from a nodal position will allow energy to be pumped into the wave.

The damping term, $\mathscr{D}$, is written as

$$\mathscr{D} = c_1\dot{\phi} + c_2\dot{\phi}\,|\,\dot{\phi}\,| + c_3\dot{\phi}^3 + \ldots \tag{19}$$

where the first two terms are likely to be sufficient if the amplitude is small. Wall friction is the main source of damping at low amplitudes, with other sources such as turbulence in the body of the bath and splashing becoming significant at high amplitudes.

For the purposes of deriving a mode evolution equation (17), assume that the effect of the gas injection on the flow field is merely to increase (or decrease) the amplitude of the fundamental and ignore any other influence of the injection on the flow. That is, the vertical plume motion and the fundamental oscillation are separate but coupled through equation (17). Also assume that, apart from the diffusion of bubbles within the plume, bubble lateral motion is a perfect response to the liquid sloshing motion. The vertical velocity of the bubbles, V_B, is taken to be independent of depth in the bath and includes a slip component relative to the liquid motion.

By considering the energy that is transferred to the wave, it is possible to show that the forcing term can be written

$$\mathscr{F} = q(Q, H, l)\int_{t-\tau}^{t} \sinh\,\kappa V_B(t-t_0)\int_{t_0}^{t'}\dot{\phi}(t') \times\cosh[\kappa z(t')]\;\mathrm{d}t'\;\mathrm{d}t_0 \tag{20}$$

where the wave number is $\kappa = \pi/l$, the transit time of bubbles through the bath is $\tau = h/V_B$, and

$$q = \frac{2\kappa^3 Qg}{\pi b\cosh\,\kappa H\sinh\,\kappa H} \tag{21}$$

An analytic solution for wave amplitude can be found from equation (20) in the usual way by assuming that ϕ is of the form

$$\phi = \phi_0\cos\,\omega t \tag{22}$$

An approximate expression for the amplitude is then

$$\phi_0 = \frac{3\pi}{8c_2\omega}\left[\frac{q(\sinh 2\kappa H - 2\kappa H)}{4(\omega^2+\kappa^2V_B^2)} + \frac{q\omega(\kappa V_B\cosh\,\kappa H\sin\,\omega\tau - \omega\sinh\,\kappa H\cos\,\omega\tau)}{(\omega^2+\kappa^2V_B^2)^2} - c_1\right] \tag{23}$$

whenever the expression is greater than zero, and zero otherwise. There is an apparent resonance (waves are most easily excited) when the transit time of bubbles through the bath, τ, is about one-half the natural wave period:

$$H/V_B \approx T/2 \tag{24}$$

The wall friction terms can be evaluated in a similar way to the forcing term after matching the potential flow solution to a boundary layer solution. This gives estimates of c_1

$$c_1^b = \frac{\kappa\sqrt{\omega\nu}}{2\cosh\,\kappa H\sinh\,\kappa H} \tag{25}$$

$$c_1^{sw} = \frac{\sqrt{\omega\nu}}{b} \tag{26}$$

and

$$c_1^{ew} = \frac{\kappa\sqrt{\omega\nu}}{\pi}\left(1 - \frac{2\kappa H}{\sinh\,2\kappa H}\right) \tag{27}$$

where c_1^b, c_1^{sw}, and c_1^{ew} are the contributions from the tank bottom, side walls, and end walls, respectively. However, these expressions are only indicative of trends, since Case and Parkinson[37] have shown that, even in the absence of gas injection, they do not predict the correct damping times if the wall surfaces are not highly polished. In practice then, the damping coefficients should be determined empirically, for example by measuring the rate of decay of an oscillation.

8. Comparison of the wave model with experiment

Whalley and Davidson[38] measured the amplitude of waves excited by gas injection in a rectangular tank 10 cm wide and 40 cm long. Air was blown through five holes distributed along a line across the tank 20 cm from either end (i.e., halfway). In a second experiment, injection was through two lines of nozzles 10 cm from each end, thereby exciting the $n = 2$ mode. In a third experiment, the $n = 3$ mode was excited by three lines of nozzles at distances of 6.7, 20, and 33.3 cm from one end. In each experiment there were five nozzles in each line, and the flow rate through each set of five nozzles was 700 cm^3/s. The bath depth was varied and the wave amplitude measured as a function of depth.

In calculating the wave amplitude (equation [23]), damping coefficients are required. The coefficient c_1 is taken to be proportional to the theoretical value, $c_1^b + c_1^{sw} + c_1^{ew}$, and the coefficient c_2 is taken to be proportional to c_1. The proportionality constants are chosen to fit the maximum amplitudes. The gas velocity is taken to be a function of bath depth based approximately on data from the literature[26]:

$$V_B = V_\infty + V_0(H_0/H)^{0.2}\quad H \geqslant 0.1$$
$$V_B = 0.54\quad H < 0.1 \tag{28}$$

with $V_\infty = 0.21$ m/s, $V_0 = 0.31$ m/s, and $H_0 = 0.15$ m.

Comparison of predicted and measured wave amplitude is given in *Figure 8*. The absolute value has effectively

been fitted (by fitting the damping constants), but the shape of the resonance curves and the range of depths over which wave motion is excited is an actual prediction of the model. The agreement in these quantities is seen to be excellent. In particular, the higher modes are excited for smaller bath depths than those at which the fundamental is excited, and this is a general prediction of the model.

The wave amplitude has also been obtained by numerically integrating equations (17) and (20).[39] This not only gives a more accurate result for finite amplitude waves but also allows the bubble velocity to vary with height in the bath. Part of this numerical integration is really equivalent to tracking the bubble motion. Insight can be gained by plotting the plume position determined in this way at a

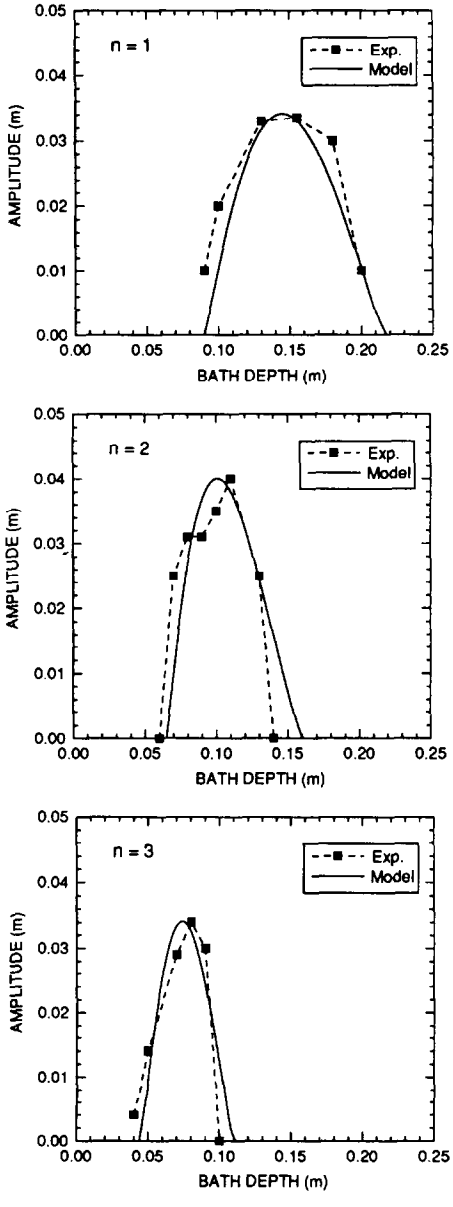

Figure 8. Predicted sloshing amplitude for the three lowest modes, compared with data of Whalley and Davidson[38].

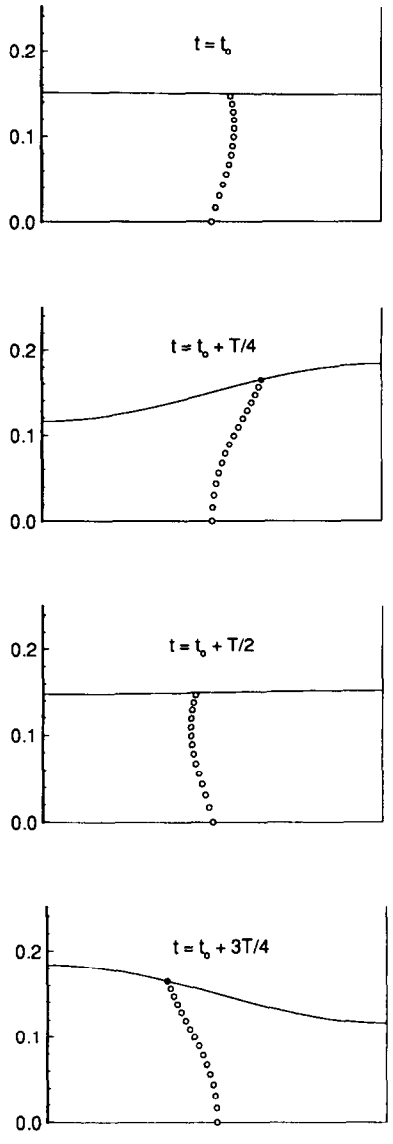

Figure 9. Four snapshots of the computed plume and surface shape over one wave period, for the $n = 1$ experiment of Whalley and Davidson[38].

sequence of different times. *Figure 9* shows four snapshots over one wave cycle showing the plume centerline position and the bath surface. In this case, the experiment with a single row of nozzles is modelled, and $H = 0.15$ m. It should be observed that the plume motion appears to lead the wave. For example, when the surface is flat the plume has already moved significantly to the rising side of the bath.

The mathematical model outlined previously can be modified to suit other simple geometries. The geometry relevant to many pyrometallurgical processes, the upright cylinder, is particularly interesting because the wave rotates (or precesses) around the vessel. This motion can be explained in terms of two degenerate nonrotating modes at right angles to each other and 90° out of phase.[35]

9. Conclusions

Mathematical models have been described for simulating three aspects of the flow dynamics of gas-injected melts. First, a two-fluid model has been shown to predict bath recirculation and bubble plume structure reasonably accurately given the complexity of the interphase interactions, i.e. interphase friction, interphase diffusion, and two-phase turbulence modification. At present semiempirical expressions for these interactions have been used. Expressions for these interactions become more uncertain as the gas flow rate is increased.

Second, the swelling where the gas plume reaches the bath surface has been simulated by two techniques: by including the gas space above the bath in the two-fluid computational domain and by deforming the boundary of the computational domain. While the first technique appears to predict the correct swelling height, the bath velocities can be adversely affected by spurious motion induced at the bath surface.

Third, a mathematical model has been described for predicting wave motion excited by gas injection into liquid baths. According to the model, the buoyancy force on bubbles that are displaced from the centerline as a result of the oscillation is sufficient to sustain the oscillation under certain conditions. This leads to a resonance-like phenomenon near

$$\tau = H/V_B = T/2 \tag{29}$$

where τ is the bubble travel time, and T is the wave period. This implies that wave motion is only excited for certain ranges of bath depth, as found experimentally.

Acknowledgment

The author would like to acknowledge the support of the HIsmelt Corporation.

Nomenclature

b	Tank width
c_1, c_2, c_3	Damping coefficients defined by equation (19)
C_1, C_2, C_μ	Empirical constants in the k-ϵ model
C_b	Coefficient in equation (14) for bubble-induced turbulence
C_f	Interphase friction coefficient
C_l	Lift coefficient in equation (7)
D_a	Additional bubble diffusivity
D_t	Turbulent diffusivity
$\mathscr{D}$	Damping term
F_f	Interphase friction force
F_l	Lift force
$\mathscr{F}$	Forcing term
g	Acceleration due to gravity
G_k	Generating function for turbulence energy
H	Bath depth
k	Kinetic energy of turbulence
l	Tank length
n	Mode number (= 1, 2, 3,...)
p	Pressure
q	Function defined by equation (21)
Q	Gas flow rate at NTP
r	Radial co-ordinate
R_g, R_l	Gas, liquid volume fraction
S_ϕ	Source term for variable ϕ
t	Time
T	Period of wave
$\mathbf{v}_l = (V_l, W_l)$	Liquid vector velocity
$\mathbf{v}_g = (V_g, W_g)$	Gas vector velocity
V_g, V_l	Gas, liquid radial velocity component
V_B	Bubble velocity
W_g, W_l	Gas, liquid vertical velocity component
z	Vertical coordinate
ϵ	Dissipation rate of turbulence kinetic energy
κ	Wavenumber
ϕ	Variable solved for
μ_{eff}, μ_l, μ_t	Effective, laminar, turbulent viscosity
ω	Angular frequency
ν	Kinematic viscosity
ν_{eff}	Kinematic effective eddy viscosity
ϕ	Mode amplitude
ρ_g, ρ_l	Gas, liquid density
σ_ϕ	Prandtl number for variable ϕ
τ	Bubble transit time through the bath

References

1. Kellogg, H. H. and Diaz, C. Bath smelting processes in non-ferrous pyrometallurgy. *Savard/Lee International Symposium on Bath Smelting*, ed. J. K. Brimacombe et al., TMS/AIME, 1992, pp. 39–65
2. Wright, J. K., Taylor, I. F. and Philp, D. K. A review of progress of the development of new ironmaking technologies. *Miner. Eng.* 1991, **4**, 983–1001
3. Cusack, B. L., Hardie, G. J. and Burke, P. D. HIsmelt—2nd generation direct smelting. *2nd European Ironmaking Conference*, Glasgow, 1991
4. Hardie, G. J., Cross, M., Batterham, R. J., Davis, M. and Schwarz, M. P. The role of mathematical modelling in the development of the HIsmelt process. *Proceedings of the 10th Process Technology Division Conference, ISS/AIME*, 1992, pp. 109–121
5. Ishii, M. and Zuber, N. Drag coefficient and relative velocity in bubbly, droplet or particulate flows. *AIChE J.* 1979, **25**, 843–855
6. Kato, Y., Nozaki, T., Nakanishi, K., Fujii, T. and Emi, T. Model study of gas-liquid momentum transfer to design optimum tuyere dimension for bottom and top/bottom blown converters. *Tetsu-to-Hagané* 1984, **70**, 380–387
7. Taylor, I. F. Gas blowthrough of liquid metal bath by an upward directed submerged jet. *ISIJ Int.* 1993, **33**, 748–756
8. Pinczewski, W. V. and Fell, C. J. D. Nature of the two-phase dispersion on sieve plates operating in the spray regime. *Trans. Inst. Chem. Eng.* 1974, **52**, 294–299
9. Zhao, Y.-F. and Irons, G. A. The breakup of bubbles into jets during submerged gas injection. *Metall. Trans. B* 1990, **21B**, 997–1003
10. Taylor, I. F., Dang, P., Schwarz, M. P. and Wright, J. K. An improved method for the experimental validation of numerical mixing time predictions. *1989 Steelmaking Conference Proceedings*, Chicago, 1989, pp. 505–516
11. Harlow, F. H. and Amsden, A. A. Numerical calculation of multiphase fluid flow. *J. Comput. Phys.* 1975, **17**, 17–52

12. Johansen, S. T. and Boysan, F. Fluid dynamics in bubble stirred ladles: Part II. Mathematical modelling. *Metall. Trans. B* 1988, **19B**, 755–764
13. Grevet, J. H., Szekely, J. and El-Kaddah, N. An experimental and theoretical study of gas bubble driven circulation systems. *Int. J. Heat Mass Trans.* 1982, **25**, 487–497
14. Sahai, Y. and Guthrie, R. I. L. Hydrodynamics of gas stirred melts: Part II. Axisymmetric flows. *Metall. Trans. B*, 1982, **13B**, 203–211
15. Stewart, H. B. and Wendroff, B. Two-phase flow: Models and methods. *J. Comput. Phys.* 1984, **56**, 363–409
16. Hinata, S., Kuga, O., Kobayasi, K. and Inoue, T. Diffusion of bubbles in two-phase flow — 2nd report: Diffusion of a single bubble and eddy diffusivity of heat in single-phase turbulent flow. *Bull. JSME* 1979, **22**, 841–847
17. Thomas, N. H., Auton, T. R., Sene, K. and Hunt, J. C. R. Entrapment and transport of bubbles by transient large eddies in multiphase turbulent shear flows. *International Conference on Physical Modelling of Multiphase Flow*, Coventry, UK, 1983, pp. 169–182
18. Davidson, M. R. Numerical calculations of two-phase flow in a liquid bath with bottom gas injection: The central plume. *Appl. Math. Model.* 1990, **14**, 67–76
19. Clift, R., Grace, J. R. and Weber, M. E. *Bubbles, Drops and Particles*. Academic Press, 1978
20. Launder, B. E. and Spalding, D. B. The numerical computation of turbulent flows. *Comput. Meth Appl. Mech. Eng.* 1974, **3**, 269–289.
21. Rosten, H. I., Spalding, D. B. and Tatchell, D. G. PHOENICS: A general-purpose program for fluid-flow, heat transfer and chemical reaction processes. *Proceedings of the 3rd International Conference on Engineering Software*, 1983, pp. 639–655
22. Rodi, W. *Turbulence Models and their Application in Hydraulics*. IAHR, Delft, Netherlands. 1980
23. Cross, M., Markatos, N. C. and Aldham, C. Gas injection in ladle metallurgy. *Control '84: Proceedings of the 1st International Symposium on Automatic Control in Mineral Processing and Process Metallurgy*, ed. J. A. Herbst, AIME-SME, 1984, pp. 294–297
24. Schwarz, M. P. and Turner, W. J. Applicability of the standard k-ϵ turbulence model to gas-stirred baths. *Appl. Math Model.* 1988, **12**, 273–279
25. Schwarz, M. P., Musgrove, A. R., Hooper, J. D. and Dang, P. Validation of numerical simulation of gas driven bath circulation by LDV measurements. *Proceedings of the 10th Process Technology Division Conference, ISS / AIME*, 1992, pp. 123–132
26. Castillejos, A. H. and Brimacombe, J. K. Measurement of physical characteristics of bubbles in gas-liquid plumes: Part II. Local properties of turbulent air–water plumes in vertically injected jets. *Metall. Trans. B* 1987, **18B**, 659–671
27. Schwarz, M. P. Two and three dimensional models of a gas-stirred bath of molten pig iron. *PHOENICS J.* 1989, **1**, 282–310
28. Sahajwalla, V., Castillejos, A. H. and Brimacombe, J. K. The spout of air jets upwardly injected into a water bath. *Metall. Trans. B* 1990, **21B**, 71–80
29. Castillejos, A. H. and Brimacombe, J. K. Measurement of physical characteristics of bubbles in gas-liquid plumes: Part I. An improved electroresistivity probe technique. *Metall Trans B* 1987, **18B**, 649–658
30. Anagbo, P. E. and Brimacombe, J. K. Plume characteristics and liquid circulation in gas injection through a porous plug. *Metall. Trans.* 1990, **21B**, 637–648
31. Turkoglu, H. and Farouk, B. Effect of gas injection velocity on mixing and heat transfer in molten steel baths. *Num. Heat Transfer, Part A*, 1992, **21**, 377–399
32. Leroy, P. and Cohen de Lara, G. Etude hydrodynamique, fondamentale et pratique, des mouvements du bain au convertisseur soufflant par le fond. *Revue de Métallurgie* 1958, **LV(2)**, 186–200
33. Schwarz, M. P., Zughbi, H. D., White, R. F. and Taylor, R. N. Flow visualization and numerical simulation of liquid bath agitation by bottom blowing. *CHEMECA 88*, University of Sydney, Sydney, Australia. 1988, pp. 537–542
34. Schwarz, M. P. Self-excited waves in gas-agitated baths. *10th Australasian Fluid Mechanics Conference*, University of Melbourne, Parkville, Australia. ed. A. E. Perry et al., 1989, pp. 3:29–3:32
35. Schwarz, M. P. Sloshing waves formed in gas-agitated baths. *Chem. Eng. Sci.* 1990, **45**, 1765–1777
36. Lamb, H. *Hydrodynamics*. Dover, New York, 1932
37. Case, K. M. and Parkinson, W. C. Damping of surface waves in an incompressible liquid. *J. Fluid Mech.* 1957, **2**, 172–184
38. Whalley, P. B. and Davidson, J. F. Self-excited oscillations in bubble columns. *VDI Berichte* 1972, **182**, 63–70
39. Schwarz, M. P. An improved model for wave excitation in liquid baths with gas injection. *11th Australasian Fluid Mechanics Conference*, eds. M. R. Davis and G. J. Walker, University of Tasmania, Hobart, Australia. 1992, pp. 207–210.